Optik 125 (2014) 2454–2457

Contents lists available at ScienceDirect

Optik

journal homepage: www.elsevier.de/ijleo

Optimized design of multiport optical circulator

Fan-Hsi Hsu [a], Jing-Heng Chen [b,*], Kun-Huang Chen [c], Chien-Hung Yeh [d,e], Ken Y. Hsu [a]

[a] Department of Photonics and Institute of Electro-Optical Engineering, National Chiao-Tung University, 1001, University Road, Hsinchu 30010, Taiwan
[b] Department of Photonics, Feng Chia University, 100, Wenhwa Road, Seatwen, Taichung 40724, Taiwan
[c] Department of Electrical Engineering, Feng Chia University, 100, Wenhwa Road, Seatwen, Taichung 40724, Taiwan
[d] Information and Communications Research Laboratories, Industrial Technology Research Institute (ITRI), Hsinchu 31040, Taiwan
[e] Graduate Institute of Applied Science and Engineering, Fu Jen Catholic University, New-Taipei 24205, Taiwan

ARTICLE INFO

Article history:
Received 27 May 2013
Accepted 24 October 2013

Keywords:
Optical circulator
Polarizing beam-splitter cube
Faraday rotator
Polarization

ABSTRACT

This research proposes a practical multiport optical circulator design by using polarizing beam splitter cubes as spatial walk-off polarizers. The use of Porro prisms for directing light requires fewer components and improves space-efficiency. Therefore, a high performance device can be produced at a reduced cost. A six-port optical circulator prototype was fabricated to show the feasibility of the proposed design. The insertion losses range between 0.52 and 1.05 dB, the isolations range between 26.20 and 45.13 dB, and the return losses are 27.72 dB. The benefits of this design's simple and symmetrical structure include cost-efficiency, simple fabrication processes, polarization-independence, the resolve of polarization-mode dispersion issues, and high performance. Additionally, the number of ports can be increased easily.

1. Introduction

Optical circulators are critical non-reciprocal devices that direct a light unidirectionally from one port to another. They are essential components for constructing fundamental network modules, such as optical add-drop multiplexers, dispersion–compensation, tunable fiber lasers, optical amplifiers, and time-domain reflectometry [1–9].

The practicality of a device is improved by high performance and cost-efficiency. In most designs, optical circulators consist of spatial walk-off polarizers (SWPs), Faraday rotators (FRs), half-wave plates (Hs), polarizing beam splitter cubes (PBSs), and various reflection prisms (RPs). The combination of FRs and Hs breaks the time-reversal symmetry that constructs the most important feature of an optical circulator. SWPs and FRs work with Hs to manipulate polarized lights in a device and are usually the most expensive parts. To be a practical device, the function of applied key components should be enhanced, the applied region on components should be space-efficient, and the number of applied components should be minimized. SWPs are critical components in the design of optical circulators and influence the device performance and cost directly. SWPs split an optical beam into two orthogonally polarized beams of which numerous implementation methods have been proposed. These methods divide optical circulators into four types: crystal, waveguide, holographic, and PBS. Crystal optical circulators use birefringent crystals as SWPs [10–13]. However, the use of birefringent crystals is hindered by challenges of highly optical qualities, crystal manufacturing, and difficult optical fabrication processes. Therefore, they are expensive. Limited by the finite birefringence, the beam splitting distance is minute; therefore, it is difficult to reduce the device length. Waveguide optical circulators use a waveguide Mach–Zehnder interferometer to implement the function of SWPs [14]. The waveguide design simplifies integration and light coupling. However, the device length is similarly difficult to shorten because of the limitations of high quality opto-magnetic materials. The holographic optical circulators are novel devices that apply polarization-selective substrate-mode volume holograms (PSVHs) to replace traditional crystal SWPs [15–18]. Although the PSVHs have the advantages of high efficiency, a level surface, compact size, and large polarization-beam splitting angles, the commercialization of these devices is limited by the availability of high-performance holographic recording materials. Conversely, PBS optical circulators use a pair of PBSs and RPs to produce the function of SWPs [19–21]. The introduction of PBSs has reduced the cost significantly and allowed the shortening of devices. However, these designs require optimization by decreasing the number and enhancing the space-efficiency of applied components. As the design of optical communication systems becomes more complex, a high performance and low cost multiport device becomes desirable.

Therefore, this research proposes a practicable multiport optical circulator design for a device with $(4+2m)$ ports that requires one FR, one H, two PBSs, two RPs, and m Porro prisms (where m is a positive integer). The introduction of the Porro

* Corresponding author. Tel.: +886 4 24517250x5093; fax: +886 4 24510182.
E-mail address: jhchen@fcu.edu.tw (J.-H. Chen).

0030-4026/$ – see front matter © 2014 Elsevier GmbH. All rights reserved.
http://dx.doi.org/10.1016/j.ijleo.2013.10.119

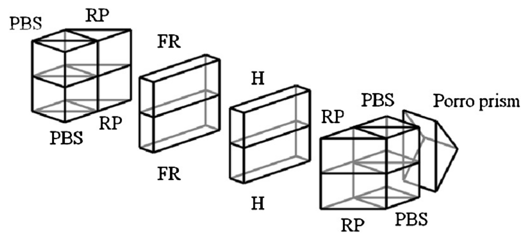

Fig. 1. Structure and components of a six-port optical circulator.

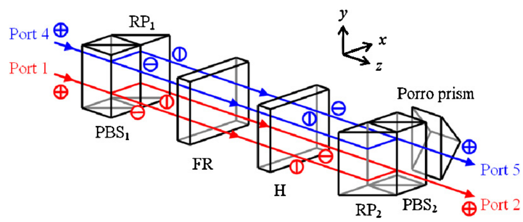

Fig. 2. Structure and operation principle of a six-port optical circulator for routes of port 1 → port 2 and port 4 → port 5.

prism for light guiding allows light propagation paths to be folded within the device. Consequently, a two-stage structure can be achieved with only one FR and the applied region on the FR window is space-efficient. To show the feasibility of the design, a six-port optical circulator prototype was assembled and tested. The benefits of the proposed design include cost-efficiency, simple fabrication processes, polarization-independence, the resolve of polarization-mode dispersion (PMD) issues, and high performance. Furthermore, the number of ports can be increased easily.

2. Principle

The structure and operation principle for the proposed multi-port optical circulator, in case of a six-port device, are shown in Figs. 1–5. Fig. 1 shows the six-port device is conceptually constructed of two stacked spatial- and polarization-modules (SPMs), and one Porro prism. The SPMs consist of a 45° FR, a 45° H, two PBSs, and two RPs. The stacked SPMs can share the same FR, H, PBS, and RP in a device (i.e. only one SPM is required, as shown in Figs. 2–5).

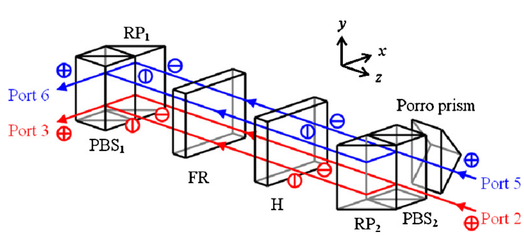

Fig. 3. Structure and operation principle of a six-port optical circulator for routes of port 2 → port 3 and port 5 → port 6.

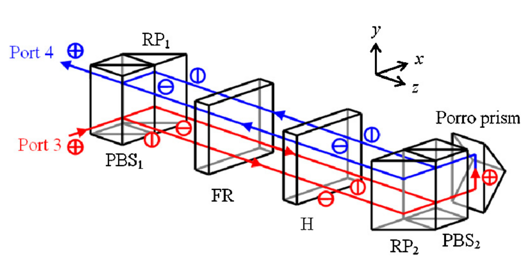

Fig. 4. Structure and operation principle of a six-port optical circulator for route of port 3 → port 4.

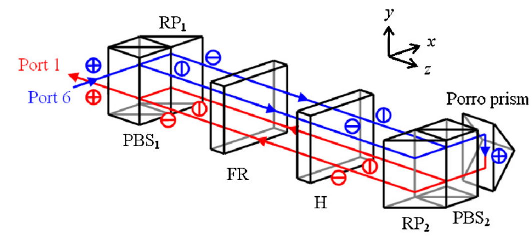

Fig. 5. Structure and operation principle of a six-port optical circulator for route of port 6 → port 1.

An x–y–z coordinate system is introduced to simplify the device description. The ⊕ symbol represents the unpolarized light, whereas symbols ⊖ and ⊖ represent p- and s-polarized lights, respectively. Fig. 2 shows the route of port 1 → port 2. An unpolarized incident light from port 1 enters PBS_1 at the lower-level of the SPM in the +z direction. The p-polarized light transmits through PBS_1 directly, whereas the s-polarized light is reflected by PBS_1 and then by RP_1. These two orthogonally polarized lights then pass through the 45° FR and the 45° H. Therefore, their states of polarization (SOPs) rotate 90° in total. Following this, they respectively enter RP_2 and the PBS_2 before they are recombined in the lower-level of the SPM. Finally, the transmitted unpolarized light enters port 2. The route from port 4 → port 5 is based on the same principle, although the transmission lights are propagated through the upper-level of the SPM, as shown in Fig. 2.

Fig. 3 shows the route of port 2 → port 3. When an unpolarized incident light from port 2 enters the PBS_2 at the lower-level of the SPM in the −z direction, the p-polarized light transmits through PBS_2 directly, whereas the s-polarized light is reflected by the PBS_2 and then by the RP_2. These two orthogonally polarized lights then sequentially pass through the 45° H and the 45° FR. Their SOPs are rotated −45° by the H and +45° by the FR. Because the FR is a nonreciprocal element, their SOPs are rotated 0° in total. The transmitted s- and p-polarized lights are recombined by PBS_1 and RP_1 in the lower-level of the SPM. Finally, the transmitted unpolarized light enters port 3 in the −x direction. The route of port 5 → port 6 is also based on the same principle. The transmission lights are propagated in the upper-level of the SPM, as shown in Fig. 3.

Fig. 4 shows the route of port 3 → port 4. An unpolarized incident light from port 3 enters PBS_1 at the lower-level of the SPM in the +x direction. The p-polarized light transmits through PBS_1 directly before being reflected by RP_1, whereas the s-polarized light is reflected by PBS_1. Following the above principle, the p- and s-polarized lights combine in the lower-level of the SPM and enter the Porro prism in the +x direction. The Porro prism then directs the lights to PBS_2 in the upper-level of the SPM in the −x direction before they finally enter port 4.

The route of port 6 → port 1 is also based on the same principle (Fig. 5). Accordingly, a polarization-independent six-port optical circulator is obtained.

3. Experimental results and discussion

A six-port optical circulator prototype with one FR (LCAFR-10-633SS, XAOT Inc.), one quartz H (WPMH05M-633, THORLABS), two BK7 PBSs, two BK7 RPs, and one Porro prism was assembled to show the feasibility of the proposed design. The FR is composed of a magnetic optical glass rod with a Verdet constant of 96 rad/T m at 632.8 nm, and is surrounded by a magnet ring with a magnetic field strength of 0.52 T at the center. The dimensions of inner diameter × outer diameter × thickness for the magnet ring are 10 mm × 42 mm × 20 mm. The dimensions of the device, including all the elements, are 41 mm × 60 mm × 60 mm. An He–Ne laser with a wavelength of 632.8 nm was used as a test light source.

Table 1
Associated losses and isolations (in Decibels).

Input port	Output port					
	1	2	3	4	5	6
1	27.72[a]	0.52[b]	38.76	32.39	38.76	32.56
2	32.56	27.72[a]	1.05[b]	38.76	45.13	26.20
3	38.76	35.13	27.72[a]	0.52[b]	26.20	35.13
4	32.39	38.76	32.56	27.72[a]	0.52[b]	38.76
5	38.76	45.13	26.20	32.56	27.72[a]	1.05[b]
6	0.52[b]	26.20	35.13	38.76	35.13	27.72[a]

All values without a superscript are isolations.
[a] Return losses.
[b] Insertion losses.

The characteristic parameters can be estimated from the measured results of each component. Table 1 shows that the insertion losses range between 0.52 and 1.05 dB, the isolations range between 26.20 and 45.13 dB, and the return losses are 27.72 dB. These results show the function of the device successfully.

The insertion losses for the port 3 → port 4 and port 6 → port 1 routes have double the value of others because of their two-stage structure. Because the crosstalk between ports 1 and 3, and 4 and 6 is caused primarily from nearby surface reflections, the isolation is less than those between other ports. The crosstalk can be reduced by an anti-reflection coating on the element surfaces and by adjusting the beams propagation directions. The orthogonally *s*- and *p*-polarized lights experience the same optical path length (OPL) for all routes (port 1 → port 2, port 2 → port 3, port 3 → port 4, port 4 → port 5, port 5 → port 6, and port 6 → port 1) because of the symmetrical and structure (Figs. 2–5). Accordingly, the device is polarization-independent and the PMD problem is resolved. When the device assembly tolerance is less than 20 μm, the PMD can be reduced to below 0.1 ps.

Compared to previous research [13,16–18,20,21], the proposed design is superior in performance and cost-efficiency. This design is used to produce a device with $(4+2m)$ ports and requires one FR, one H, two PBSs, two RPs, and m Porro prisms (where m is a positive integer). Because PBSs and RPs are introduced to as SWPs, the implementation of the device is highly practicable and is not limited by practical birefringent crystals [13] and holographic recording materials [16–18]. Due to the introduction of Porro prism for light guiding, light beams propagate in three dimensions and light propagation paths are folded in the device. Consequently, only one FR and a minimum of components are required for the assembly of this design. Conversely, two FRs and several components are required for the assembly of other multiport optical circulators designs. Fewer components for assembly implies a reduced cost, compact size, robust design, low insertion loss, and a simple assembly process. Fig. 6 shows (not to scale) that the number of ports can be increased by two if an additional Porro prism is added to the system. However, other designs require significantly more components to achieve identical results [13,16,17,20,21]. The introduced Porro prisms are positioned on Side A and Side B to direct light between layers $2m-1$ and $2m$, and between layers $2m$ and $2m+1$ (where m is a positive integer). However, the practicability could be limited by the actual size of the transmission window of an FR.

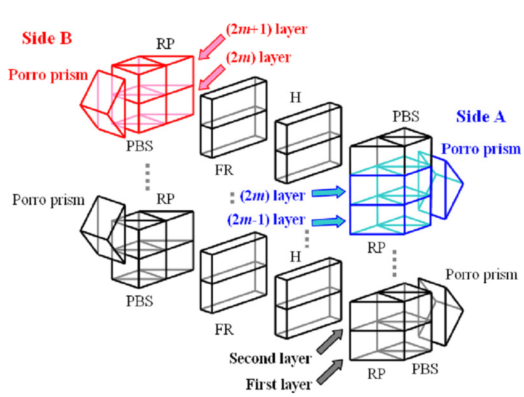

Fig. 6. Schematic representation of introduction of Porro prism for a multiport optical circulator.

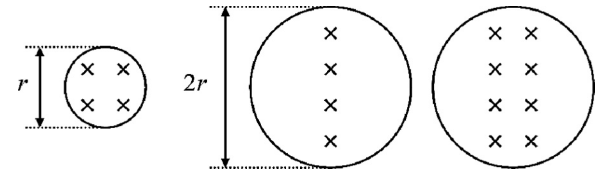

Fig. 7. Light passing through positions on an FR window for (a) the proposed six-port device design, (b) a six-port device in our previous work [21], and (c) a 10-port device using the proposed design.

Additionally, the cost of an FR depends on its transmission window size (i.e. the cross section of magnetic optical glass rod). Fig. 7 shows comparisons between this design and previous research [21] on the light passing through various positions of an FR window. Fig. 7(a) and (b) compares the FR window usage region of a six-port device with a previous design. The FR window of the six-port device is concentrated centrally and requires an area of one quarter of the FR window (radius r), and is therefore more space-efficient than previous design. This shows the cost-effectiveness of the proposed design. A comparison between Fig. 7(b) and (c) shows that the same area of an FR window (radius $2r$) for a six-port device in previous research can support a 10-port device using the proposed design.

A 632.8 nm He–Ne laser was applied as a test light source for the alignment and measurement. Consequently, the operation wavelength can be designed at 830, 1300, or 1550 nm for optical communications.

4. Conclusions

This research proposed an optimized multiport optical circulator design by using PBSs as SWPs. The introduction of the Porro prisms allows a minimum of required assembly elements, thus improving the space-efficiency of the device. A six-port optical circulator prototype was fabricated and tested to show the feasibility of the design. The advantages of this design include high practicability and simple fabrication processes, high performance and cost-efficiency, polarization independence, the resolving of polarization mode dispersion, and the ability to increase the number of ports easily.

Acknowledgement

This work was partly supported by the National Science Council, Taiwan, ROC, under Contract Nos. NSC 101-2221-E-035-053 and NSC 100-2632-E-035-001-MY3.

References

[1] D.K. Mynbaev, L.L. Scheiner, Fiber-Optic Communications Technology, Prentice Hall, New Jersey, 2001 (chapter 6).
[2] Y.K. Chen, C.J. Hu, C.C. Lee, K.M. Feng, M.K. Lu, C.H. Chang, Y.K. Tu, S.L. Tzeng, Low-crosstalk and compact optical add-drop multiplexer using a multiport circulator and fiber Bragg gratings, IEEE Photon. Technol. Lett. 12 (10) (2000) 1394–1396.
[3] A.V. Tran, C.J. Chae, R.S. Tucker, A bidirectional optical add-drop multiplexer with gain using multiport circulators, fiber Bragg gratings, and a single unidirectional optical amplifier, IEEE Photon. Technol. Lett. 15 (7) (2003) 975–977.

[4] T. Komukai, Y. Miyajima, M. Nakazawa, An in-line optical bandpass filter with fiber gratings and an optical circulator and its application to pulse-compression, Jpn. J. Appl. Phys. 34 (1995) L230–L232.
[5] H. Lin, C.H. Chang, High power C + L-band Erbium ASE source using optical circulator with double-pass and bi-directional pumping configuration, Opt. Express 12 (25) (2004) 6135–6140.
[6] M. Yamada, M. Shimizu, Y. Ohishi, J. Temmyo, T. Kanamori, S. Sudo, Highly efficient configuration of a pr^{3+}-doped fluoride fiber amplifier module with an optical circulator, IEEE Photon. Technol. Lett. 5 (9) (1993) 1011–1013.
[7] Y. Sato, K. Aoyama, OTDR in optical transmission systems using Er-doped fiber amplifiers containing optical circulators, IEEE Photon. Technol. Lett. 3 (11) (1991) 1001-1003.
[8] C.H. Yeh, C.C. Lee, C.Y. Chen, S. Chi, A stabilized and tunable erbium-doped fiber ring laser with double optical filter, IEEE Photon. Technol. Lett. 16 (3) (2004) 765–767.
[9] S.K. Liaw, W.Y. Jang, C.J. Wang, K.L. Hung, Pump efficiency improvement of a C-band tunable fiber laser using optical circulator and tunable fiber gratings, Appl. Opt. 46 (12) (2007) 2280–2285.
[10] M. Koga, T. Matsumoto, Polarisation-insensitive high-isolation nonreciprocal device for optical circulator application, Electron. Lett. 27 (11) (1991) 903–905.
[11] Y. Fujii, Compact high-isolation polarization-independent optical circulator, Opt. Lett. 18 (3) (1993) 250–252.
[12] L.D. Wang, High-isolation polarization-independent optical quasi-circulator with a simple structure, Opt. Lett. 23 (7) (1998) 549–551.
[13] J.H. Chen, K.H. Chen, H.Y. Hsieh, F.H. Hsu, Design of crystal type multi-port optical quasi-circulator, IEEE Photon. Technol. Lett. 22 (1) (2010) 48–50.
[14] N. Sugimoto, T. Shintaku, A. Tate, H. Terui, M. Shimokozono, E. Kubota, M. Ishii, Y. Inoue, Waveguide polarization-independent optical circulator, IEEE Photon. Technol. Lett. 11 (3) (1999) 355–357.
[15] J.H. Chen, K.H. Chen, D.C. Su, Holograms-Recording Materials and Applications, INTECH (2011) (chapter 12).
[16] J.H. Chen, P.J. Hsieh, J.Y. Lin, D.C. Su, Improved N-port optical quasi-circulator by using a pair of orthogonal holographic spatial- and polarization-modules, Opt. Express 12 (26) (2004) 6553–6558.
[17] J.H. Chen, P.J. Hsieh, D.C. Su, J.C. Su, Multi-port polarization-independent optical quasi-circulators by using a pair of holographic spatial- and polarization-modules, Opt. Express 12 (4) (2004) 601–608.
[18] J.H. Chen, D.C. Su, J.C. Su, Holographic spatial walk-off polarizer and its application to a 4-port polarization-independent optical circulator, Opt. Express 11 (17) (2003) 2001–2006.
[19] H. Iwamura, H. Iwasaki, K. Kubodera, Y. Torii, J. Noda, Simple polarisation-independent optical circulator for optical transmission systems, Electron. Lett. 15 (25) (1979) 830–831.
[20] J.H. Chen, K.H. Chen, J.Y. Lin, H.Y. Hsieh, Multi-port optical circulator by using polarizing beam splitter cubes as spatial walk-off polarizers, Appl. Opt. 49 (8) (2010) 1430–1433.
[21] J.H. Chen, K.H. Chen, C.H. Yeh, W.P. Huang, Simplified design of multiport optical circulator with parallel connection of mirror-image arranged spatial- and polarization-modules, IEEE Photon. Technol. Lett. 23 (2011) 1766–1768.